

# Quaternary Rupture of a Crustal Fault beneath Victoria, British Columbia, Canada

**Kristin D. Morell**, School of Earth and Ocean Sciences, University of Victoria, Victoria, British Columbia V8P 5C2, Canada, [kmorell@uvic.ca](mailto:kmorell@uvic.ca); **Christine Regalla**, Department of Earth and Environment, Boston University, Boston, Massachusetts 02215, USA; **Lucinda J. Leonard**, School of Earth and Ocean Sciences, University of Victoria, Victoria, British Columbia V8P 5C2, Canada; **Colin Amos**, Geology Department, Western Washington University, Bellingham, Washington 98225-9080, USA; and **Vic Levson**, School of Earth and Ocean Sciences, University of Victoria, Victoria, British Columbia V8P 5C2, Canada

## ABSTRACT

The seismic potential of crustal faults within the forearc of the northern Cascadia subduction zone in British Columbia has remained elusive, despite the recognition of recent seismic activity on nearby fault systems within the Juan de Fuca Strait. In this paper, we present the first evidence for earthquake surface ruptures along the Leech River fault, a prominent crustal fault near Victoria, British Columbia. We use LiDAR and field data to identify >60 steeply dipping, semi-continuous linear scarps, sags, and swales that cut across both bedrock and Quaternary deposits along the Leech River fault. These features are part of an ~1-km-wide and up to >60-km-long steeply dipping fault zone that accommodates active forearc transpression together with structures in the Juan de Fuca Strait and the U.S. mainland. Reconstruction of fault slip across a deformed <15 ka colluvial surface near the center of the fault zone indicates ~6 m of vertical separation across the surface and ~4 m of vertical separation of channels incising the surface. These displacement data indicate that the Leech River fault has experienced at least two surface-rupturing earthquakes since the deglaciation following the last glacial maximum ca. 15 ka, and should therefore be incorporated as a distinct shallow seismic source in seismic hazard assessments for the region.

## INTRODUCTION

Unlike plate boundary faults that often exhibit a strong seismic or geodetic expression (e.g., Rogers, 1988), active faults within the adjacent crust can have long recurrence intervals (e.g., 5–15 k.y.; Rockwell et al., 2000), and they may not be

detectable by seismic or geodetic monitoring (e.g., Mosher et al., 2000; Balfour et al., 2011). This point was exemplified by the 2010  $M_w$  7.1 Darfield, New Zealand (Christchurch), earthquake and aftershocks that ruptured the previously unidentified Greendale fault (Gledhill et al., 2011). This crustal fault showed little seismic activity prior to 2010, but nonetheless produced a 30-km-long surface rupture, caused more than 180 casualties, and resulted in at least

US\$10 billion in damage (Quigley et al., 2012).

In the forearc of the Cascadia subduction zone (Fig. 1), where strain accrues due to the combined effects of northeast-directed subduction and the northward migration of the Oregon forearc block (McCaffrey et al., 2013), microseismicity data are sparse and do not clearly elucidate planar crustal faults (Cassidy et al., 2000; Balfour et al., 2011). But geomorphic,

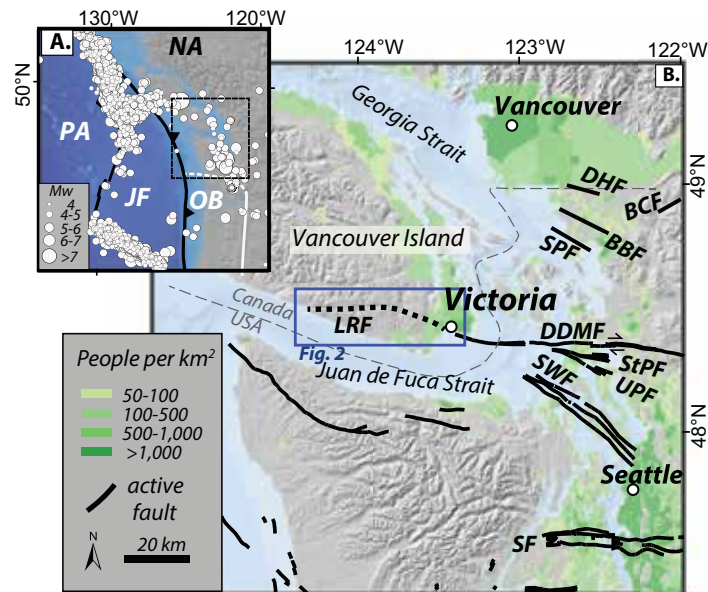
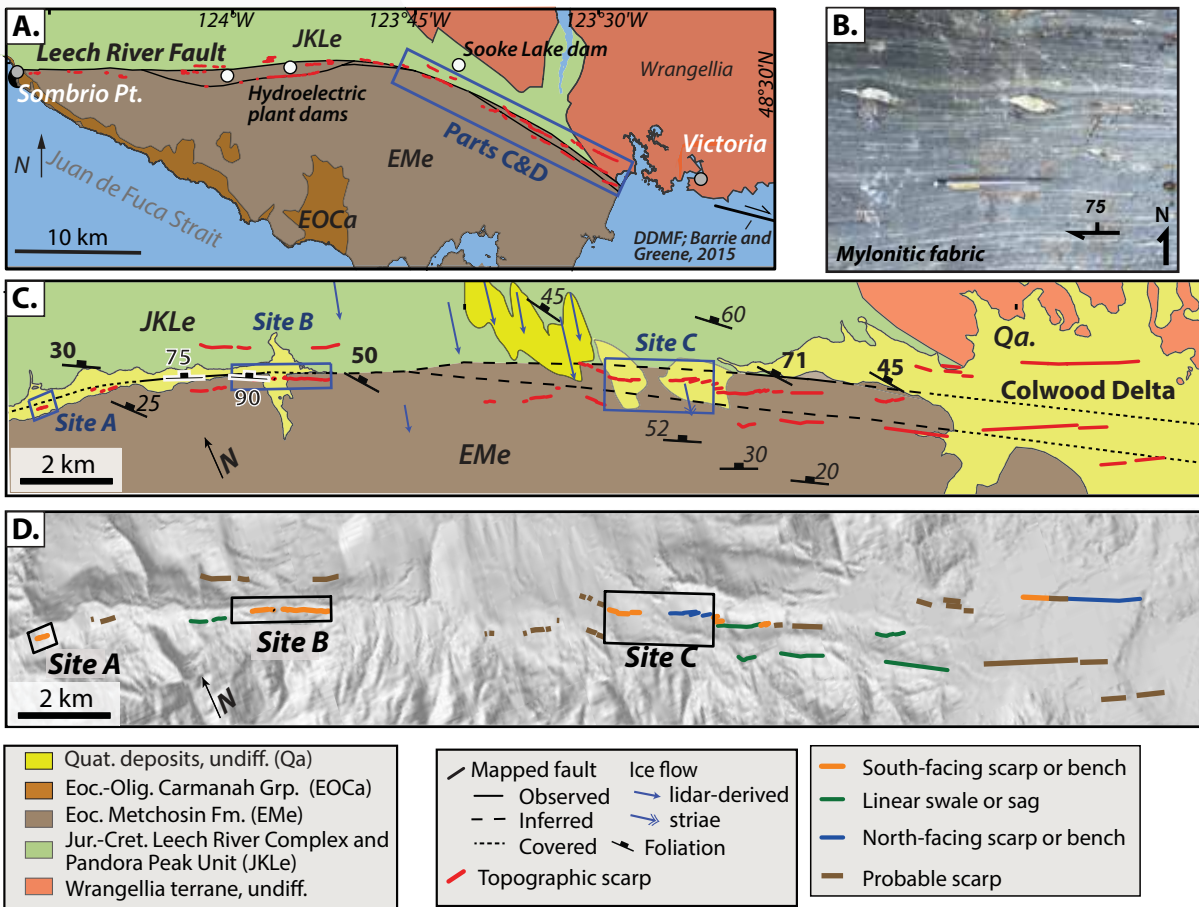


Figure 1. (A) Tectonic setting. White circles—locations of historical earthquakes (USGS NEIC) between AD 1946 and 2015, scaled by magnitude. White line—boundary between Oregon Block (OB) and North America plate (NA) (McCaffrey et al., 2013; Wells and Simpson, 2001). JF—Juan de Fuca plate; PA—Pacific plate. (B) Population centers (Balk et al., 2006) relative to mapped active faults in black (Sherrrod et al., 2008; USGS, 2010; Kelsey et al., 2012; Personius et al., 2014; Barrie and Greene, 2015). The Leech River fault (LRF) is shown as dashed line. BBF—Birch Bay fault; BCF—Boulder Creek–Canyon Creek fault; DDMF—Darrington–Devil’s Mountain fault; DHF—Drayton Harbor fault; SPF—Sandy Point fault; StPF—Strawberry Point fault; SF—Seattle fault; SWF—South Whidbey Island fault; UPF—Utsalady Point fault.



**Figure 2.** (A) Simplified geologic map of the Leech River fault and surroundings (after Massey et al., 2005). Red lines denote topographic scarps, pressure ridges, topographic benches, and linear swales and sags identified in this study. See geological legend at base of figure. DDMF—Darrington–Devil’s Mountain fault. (B) Mylonitic fabrics within the Leech River Complex near its contact with the Metchosin Fm. (C) Map showing trace of identified features relative to bedrock (Massey et al., 2005), surficial deposits (Blyth and Rutter, 1993), and local ice flow indicators (blue arrows, this study). Foliation measurements from this study are shown in bold and those from Muller (1983) are shown in italics. Foliation data outlined in white are at the lithologic contact (this study). (D) Fault traces as in part C, colored according to facing direction and feature type, draped on LiDAR hillshade image.

trenching, and geophysical studies have proven successful at highlighting a network of oblique reverse forearc faults, both on- and offshore of Washington and Oregon, that can produce earthquakes up to 7.5 in magnitude (McCaffrey and Goldfinger, 1995; ten Brink et al., 2006; Blakely et al., 2014; Sherrod et al., 2016). In particular, LiDAR, seismic, and aeromagnetic data have been paramount in the recognition of the Seattle fault as a significant seismic hazard source within the greater Seattle region (SF, Fig. 1) (Johnson et al., 1999; Blakely et al., 2002; Kelsey et al., 2008; Nelson et al., 2014).

The potential Quaternary activity of the Leech River fault, an ~60-km-long terrane-bounding fault in the southern Vancouver Island forearc (Muller, 1977; MacLeod et al., 1977), has drawn significant attention in recent years because of

the seismic hazard it may pose to the nearby population of Victoria, British Columbia (Figs. 1 and 2A) (see Cassidy et al., 2000; Mosher et al., 2000; Balfour et al., 2011). Several previous authors suggest that this fault, which places Jurassic-Cretaceous schists of the Leech River Complex to the north against Eocene basalts of the Metchosin Formation to the south (Fig. 2A) (Fairchild and Cowan, 1982; Rusmore and Cowan, 1985), was last active in the Eocene (MacLeod et al., 1977; Johnston and Acton, 2003). Yet, trenching, coring, and geophysical studies indicate multiple Quaternary ruptures of adjacent fault systems in Washington state, USA, including the Southern Whidbey Island fault, the Utsalady Point fault, and the Darrington–Devil’s Mountain fault (Fig. 1) (Johnson et al., 1996, 2001; Sherrod et al., 2008; Personius et al., 2014). Quaternary seismic

activity is also recognized 10–20 km offshore of the Leech River fault along a structure in the Juan de Fuca Strait (Barrie and Greene, 2015) (Figs. 1 and 2A), but direct evidence for recent rupture onshore has remained ambiguous.

Here, we use a combination of techniques to delineate Quaternary fault-related features along the Leech River fault, including (1) mapping of fault scarps from hillshade and local slope images generated from a high resolution (~2 m horizontal by ~10 cm vertical) LiDAR digital elevation model (DEM) collected by Natural Resources Canada (James et al., 2010); (2) first-order bedrock and surficial field mapping; (3) collection of detailed structural and geomorphic data at key sites; and (4) compilation of our observations with data from previous studies (e.g., Fairchild and Cowan, 1982; Blyth and Rutter, 1993;

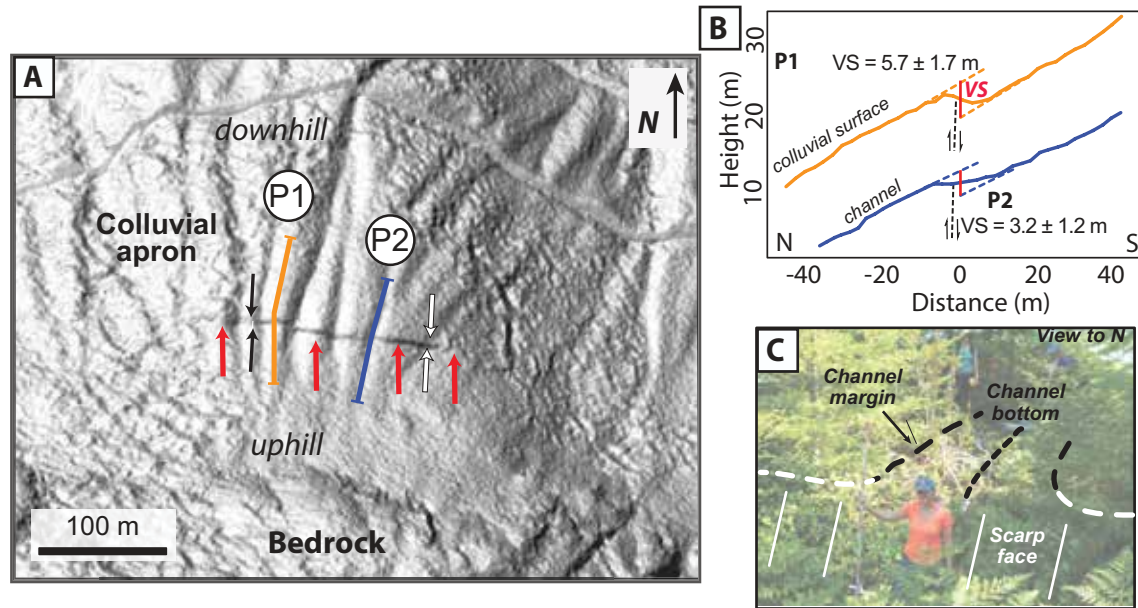


**Figure 3.** (A) LiDAR hillshade map of Site A, showing an uphill (south) facing scarp cutting the surface of a steeply north-sloping colluvial apron and channels. Red arrows point to steep face. Black and white arrows show apparent left and right (respectively) lateral separations of channel margins. Example profile lines (P1 and P2) locations shown. Additional profile lines are shown in Figure DR2 (see text footnote 1). (B) An example of LiDAR-derived elevation profiles from interfluvium P1 and channel P2. VS—vertical separation. (C) Field photo showing tectonic scarp in a channel at site C.

Massey et al., 2005). We identify several strands of the Leech River fault that displace post-glacial sediments and record at least two  $M_w > 6$  earthquakes since the Cordilleran deglaciation ca. 15 ka (Clague and James, 2002). These data provide the first evidence for Quaternary surface rupture along a crustal fault that lies within close proximity of Victoria, British Columbia, and suggest that the Leech River fault is only one of a network of active faults that accommodate forearc deformation in southwestern Canada.

## OBSERVATIONS

We mapped >60 topographic features along the Leech River fault that together extend >60 km in length and span ~1 km in width. Individual features range in length from hundreds of meters to >2.5 km, reach up to ~5 m in height, and form linear ridges, sags, and scarps with both north- and south-facing directions (Fig. 2). Along the eastern half of the fault, where we focused our analysis, these topographic features coincide with displaced geomorphic surfaces, steeply dipping brittle faults, and uphill-facing bedrock scarps.

In order to exclude topographic features that were produced by differential erosion

along steeply dipping foliation planes, we mapped the position of lithologically distinct units and collected structural data on the occurrence and orientation of foliation and fault deformation fabrics. The topographic scarps we identified are roughly parallel to the previously mapped location of the Leech River fault (Fairchild and Cowan, 1982; Massey et al., 2005), but none of the identified fault scarps coincide exactly with the fault contact between the Leech River Complex and the Metchosin Formation (Fig. 2). Instead, individual topographic features occur both north and south of the lithologic fault boundary by as much as hundreds of meters. Where a discrete contact between the basalt and schist units is exposed at two locations in the area, the fault strikes parallel to regional foliation ( $300\text{--}310^\circ$ ) but dips more steeply ( $70\text{--}90^\circ$  NE) than the foliation ( $\sim 45^\circ$  NE) (Figs. 2B and 2C, and GSA Data Repository<sup>1</sup> Fig. DR1A). The westernmost of these sites contains a 10- to >200-m-wide mylonitic shear zone within both units, but exhibits no brittle deformation at the outcrop scale (Figs. 2B and 2C). Because the mapped features do not coincide with the lithologic terrane boundary, they cannot be explained by

differential erosion across this strong lithologic contrast.

To further exclude topographic features produced by glacial processes, we determined local ice flow directions from bedrock striae and streamlined glacial deposits and collected geomorphic data designed to confirm a tectonic origin. The roughly east-west-oriented topographic features on the eastern half of the Leech River fault are nearly perpendicular to the southerly regional ice flow direction during the last glacial maximum. The LiDAR data delineate large (km-long) drumlinoid ridges with well-defined apices that are distinctively streamlined with steep up-ice (northern) margins and upper surfaces that gently slope in a southerly, down-ice direction (Figs. 2C and 2D). Our field work confirms that these ridges are mantled by glacial sediments (Fig. DR1E [see footnote 1]). South-directed ice flow is further supported by glacial striae data on bedrock near the drumlinoid ridges (Fig. 2C). The observation that the mapped scarps strike perpendicular to the ice flow direction rules out their formation by ice flow-parallel processes, including glacial scouring, grooving, molding, and streamlining.

<sup>1</sup> GSA Data Repository Item 2017046, supplementary figures, is online at <http://www.geosociety.org/datarepository/2017/>. If you have questions, please email [gsatoday@geosociety.org](mailto:gsatoday@geosociety.org).

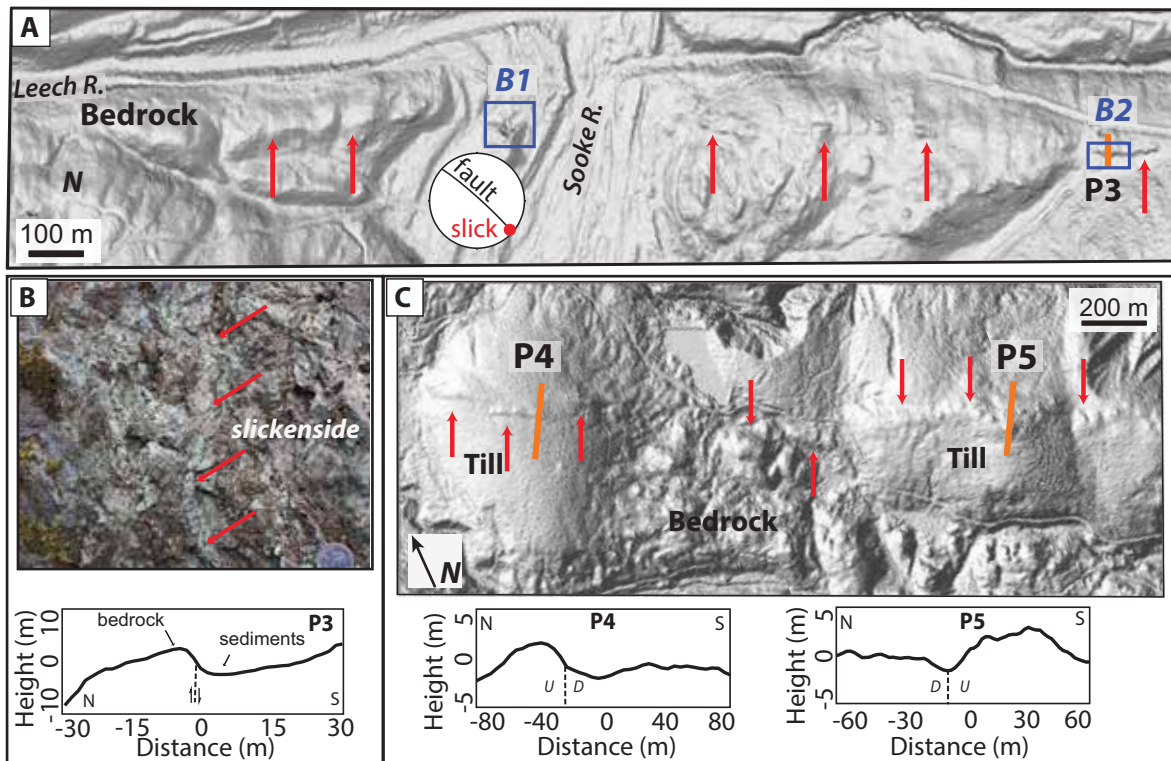


**Figure 4.** (A) LiDAR hillshade image for site B where there is a >1.5-km-long scarp in bedrock. Red arrows point to steep face. Steeonet from fault at site B1. (B) Field photo of gouge-bearing fault at site B1, with subhorizontal slickensides. Elevation profile at bottom for site B2. (C) LiDAR hillshade for site C showing topographic features with opposing facing directions and a morphology suggestive of pressure ridges. Red arrows point to the steep face. LiDAR-derived elevation profiles shown below the image. Because structures are buried beneath dense vegetation and glacial till, fault locations are inferred (dashed lines on the profiles). U and D denote up- and downthrown sides, respectively.

## FIELD EVIDENCE FOR TECTONIC SCARPS

We identify three key sites (Figs. 2C and 2D, sites A–C) where field and LiDAR data indicate tectonic displacement of bedrock and Quaternary deposits.

### Site A

Near the center of the Leech River fault, the LiDAR data reveal a >200-m-long and up to ~3–6-m-high topographic scarp that faces uphill (southward) across a relatively steep (~20°), north-facing slope (Fig. 3A). Beneath an ~1-m-thick mantle of colluvium at the surface, the hillside consists of a dense, matrix-supported diamict with numerous erratics and striated clasts, interpreted as subglacial till. These field observations, the relatively smooth surface morphology, and the lack of a fan apex, indicate that this ~400-m-long by ~300-m-wide hillside is covered by an apron of colluvium. Several steep, linear

channels littered with boulders incise this colluvial apron.

LiDAR and field data indicate that both the colluvial surface and the channels incising it are vertically displaced by several meters across the scarp (~3–6 m) (Figs. 3 and DR1B [see footnote 1]). We calculated vertical separations at 12 locations across the fault scarp by linear regression of LiDAR-derived topography and estimated regression uncertainties using a Monte Carlo routine (following Thompson et al., 2002) (Fig. DR2 [see footnote 1]). These data confirm that scarp height is systematically lower within the incised channels than on the colluvial surface. For example, at interfluvial P1, the vertical separation across the scarp approaches ~6 m ( $5.7 \pm 1.7$  m) (Fig. 3B). At channel P2, however, the LiDAR profiles indicate only ~3 m ( $3.2 \pm 1.2$  m) of vertical separation. On average, the interfluves are vertically separated by  $5.7 \pm 1.3$  m ( $n = 8$ ) and the channels by  $3.9 \pm 0.9$  m ( $n = 4$ ) ( $1\sigma$ )

(Fig. DR2). These estimates support our field observations of a differential amount of displacement across the scarp between channels versus interfluves (Fig. 3C).

Several field observations suggest this scarp reflects north-side-up dip slip displacement along a steeply north-dipping (60–90°) fault. For instance, the interaction of the scarp with local topography suggests that the fault dips steeply to the north; the scarp trace is nearly linear in map view, but it deviates slightly northward into topographic lows (Fig. DR2A). Additionally, both the apparent north-side-up displacement and the spatial pattern of channel displacement indicate dip slip displacement with little to no lateral displacement. While northeast-trending channels show apparent right separation (white arrows, Fig. 3A), north-northwest-trending channels show apparent left separation (black arrows, Fig. 3A). Together, these data indicate that both the colluvial surface and the channels have

been vertically displaced by ~4–6 m due to slip on a steep, north-dipping reverse fault.

### Site B

Five kilometers east along strike from site A, a prominent south-facing bedrock scarp extends for ~1.5 km and shows evidence for brittle deformation along its length (site B, Figs. 2 and 4). Near the center of this scarp, an abandoned rock quarry exposes two steeply north-dipping sub-parallel faults (dipping 85° to N40°E) cutting Metchosin Formation basalt (site B1, Figs. 4A and 4B). Both faults have a 1–2-mm-wide gouge zone and exhibit sub-horizontal slickenlines (05° toward 129°) consistent with strike-slip motion (Figs. 4B and DR1C [see footnote 1]). At the eastern end of site B, the scarp becomes ~4 m high and uphill facing (Fig. 4A). Here, the northern (upthrown) side of the scarp consists of fractured and brittly deformed Metchosin Formation basalt, whereas the southern (downthrown) side of the scarp contains fine-grained sediment (P3, Fig. 4B). Similar to site A, the apparent north-side-up displacement across the scarp and the northward divergence of the scarp trace into topographic lows signifies dip displacement along a steeply north-dipping reverse fault (Figs. 4B and DR1D). Overall, these observations suggest an origin for this feature as a tectonic scarp.

### Site C

Approximately 5 km east of site B, an ~1.5-km-long region contains >300-m-long ridges, linear sags, and swales up to ~2–5 m in height that cut across relatively smooth, gently sloping till-mantled hillslopes (Figs. 4C and DR1E). These topographic features display several differences from those at sites to the west. Whereas sites A and B exhibit discrete topographic scarps, features in this region are 10–15-m-wide elevated zones that sit more than ~5 m above the surrounding landscape. Moreover, while the scarps at sites A and B remain north-facing for hundreds of meters along strike, the facing direction of the features in site C transitions southeastward from south- to north-facing over a short (~200 m) distance (Figs. 2D and 4C).

These scarps have a nearly linear trace across topography, but they do not exhibit clear upthrown fault blocks or a marked

increase in surface elevation. We interpret this en echelon arrangement of topographic ridges and the lateral juxtaposition of topographic highs and lows as pressure ridges, common in strike slip or oblique slip systems (e.g., Sylvester, 1988; Sherrod et al., 2008, 2016; Nelson et al., 2014).

### QUATERNARY SLIP ON THE LEECH RIVER FAULT

The displaced geomorphic features, faulted bedrock, and prominent scarps collectively argue that several strands of the Leech River fault have been active since the late Pleistocene. Our observations support a tectonic genesis for the topographic features we identify for several reasons. First, several of the identified topographic features show evidence for extensive brittle faulting. For example, the fractured rock and gouge along the scarp at site B (Fig. 4B) require a tectonic origin and exclude formation by either ice plucking or the erosion of a bedrock foliation. Second, the observation that paleo-ice flow was directed to the south, at a high angle to the orientation of the topographic features (Fig. 2C), further rules out formation by glacial processes. Finally, it is unlikely that the topographic scarps in Quaternary deposits were produced by landslide processes. Several of the scarps, including those at sites A and B (Figs. 2C and 2D), are uphill facing, nearly perfectly linear, and do not exhibit curvilinear head scarps that would be expected for landslides.

The most compelling evidence for a tectonic origin for these topographic features comes from site A, where both the hillslope surface and multiple channels are displaced vertically along an uphill facing scarp (Figs. 3A and 3B). The scarp at site A cannot represent the remnants of an abandoned logging road or placer mining excavation because the base of the scarp is not graded, and the upper and lower surfaces are vertically separated by >~4 m (Fig. 3B). Such displacement in hillslope elevation, and in particular the displaced channels, cannot be produced by any mechanism other than fault displacement. Because the colluvial apron at this site remains both in situ and intact, the tectonic scarps crosscutting the colluvial surface and inset channels must be no older than the deglaciation following the last glacial maximum (ca. 15 ka) (Clague and James, 2002).

We suggest that the identified scarps together compose an active fault system that is up to ~1 km wide and 30–60 km long (Fig. 2A). Although individual lineaments can be traced for only hundreds of meters along strike, meter-high fault scarps are not easily preserved in this wet climate, and the fault scarps are semi-continuous with one another along strike. Our recognition of topographic features along the western ~30 km of the fault similar to those on the eastern half (Fig. 2C) suggests that the active fault zone extends the entire 60-km length of the fault onshore (Fig. 2A). Scarp morphology, fault orientations, and fault kinematics suggest that the active strands of the Leech River fault accommodate strike and dip slip motion within a steeply dipping fault zone or flower structure. Within a zone up to 1 km wide, we observe near vertical faults, variable scarp facing directions, laterally discontinuous surface scarps, and field evidence for strike-slip and reverse faulting. These characteristics are typical of strike slip systems and are similar to features observed along active oblique-reverse faults in the adjacent Pacific Northwest (e.g., Johnson et al., 2001; Sherrod et al., 2008, 2016; Kelsey et al., 2012; Nelson et al., 2014; Personius et al., 2014; Blakely et al., 2014).

These new results challenge the prevailing view that the Leech River fault was primarily an Eocene structure (cf. MacLeod et al., 1977). This interpretation was partly based on the observation that relatively undeformed Oligocene sediments of the Carmanah Group (Sooke Fm.) lie unconformably above healed fractures and mylonitic fabrics close to the trace of the Leech River fault near Sombrio Point (Fig. 2A) (MacLeod et al., 1977). However, our results from the eastern half of the Leech River fault show that active fault strands occur within a zone as much as 1 km wide and these strands are not always co-located with observed fault-related fabrics. Therefore, the location of fault fabrics may not coincide with the surface trace of the active fault.

### IMPLICATIONS FOR PALEOSEISMICITY

The displaced channels and colluvial surface at site A suggest this section of the Leech River fault has experienced at least two, and possibly three or more, large,

surface-rupturing earthquakes since the formation of the surface ca. 15 ka. For a 60–90° reverse fault, the displacements across the scarp require minimum dip displacements of  $6.4 \pm 1.5$  m for interflaves ( $n = 8$ ) and  $4.4 \pm 1.1$  m for channels ( $n = 4$ ). The ~2 m difference in displacement between the channels and interflaves implies multiple episodes of fault activity and suggests that at least one event with ~2 m displacement occurred after the formation of the colluvial apron but before channel incision. In addition to this early event, the ~4 m of displacement of the channels (Fig. 3B and DR2 [see footnote 1]) requires either one large event with ~4 m of slip, or multiple smaller events that together sum to ~4 m of slip. Global empirical relationships suggest that surface displacements on the order of meters correspond to earthquakes of  $M_w$  6 or greater (e.g., Wells and Coppersmith, 1994).

## IMPLICATIONS FOR REGIONAL SEISMOTECTONICS

Several observations indicate the active Leech River fault zone is part of a network of high-angle oblique faults that accommodate regional transpression across the Juan de Fuca Strait and Puget Sound region. Barrie and Greene (2015) trace the Devil's Mountain fault of Washington state, USA, to within 10–20 km of the fault scarps on Fig. 2, and their bathymetric and seismic surveys reveal a steeply dipping oblique-slip fault zone similar to our observations of the Leech River fault zone. Both the Darrington–Devil's Mountain fault and the Southern Whidbey Island fault systems of Washington state (Fig. 1) are likewise near-vertical fault zones with oblique slip histories (Sherrod et al., 2008; Personius et al., 2014) similar to many of the crustal fault systems throughout the Puget Sound region (e.g., McCaffrey and Goldfinger, 1995; ten Brink et al., 2006; Blakely et al., 2014; Nelson et al., 2014; Sherrod et al., 2016). Considering these similarities in orientation and slip sense, we suggest that the Leech River fault is part of this regional active forearc fault system. Although it remains possible that the timing of past ruptures along these fault systems was influenced by stress loading or release related to the last glaciation (e.g., Hetzel and Hampel, 2005), repeated earthquakes on crustal faults including the Leech River should be expected in order to accommodate

ongoing tectonic strain in the forearc of the active Cascadia subduction zone.

## IMPLICATIONS FOR SEISMIC HAZARD

The length of the active Leech River fault zone (30–60 km; Fig. 2A) and its history of multiple Quaternary ruptures suggest it is capable of producing earthquakes of  $M_w > 6$ . This active fault zone lies within tens of kilometers of downtown Victoria and in close proximity to three local water dams. One of these dams is located within 2 km of the active fault zone and supports the region's principal water supply reservoir (Fig. 2A). The other two dams lie within the active fault zone and support a hydroelectric power plant. Thus, our new identification of a significant shallow seismic source has considerable implications for the seismic risk exposure of this populated region. Surface-rupturing earthquakes with shallow hypocenters can be highly destructive, and it is therefore important that the Leech River fault zone be incorporated into seismic hazard assessments of southwestern British Columbia and neighboring regions.

## ACKNOWLEDGMENTS

We thank CRD watersheds and BC Hydro for access to key field sites. This manuscript benefited from comments by Jack Loveless, Alan Nelson, Christie Rowe, and two anonymous reviewers. We thank Steven Whitmeyer for editorial handling. This research was supported by an NSERC Discovery grant to KM and NSF EAR IRFP Grant #1349586 to CR.

## REFERENCES CITED

- Balfour, N., Cassidy, J., Dosso, S., and Mazzotti, S., 2011, Mapping crustal stress and strain in southwest British Columbia: *Journal of Geophysical Research: Solid Earth* (1978–2012), v. 116, B03314, doi: 10.1029/2010JB008003.
- Balk, D., Deichmann, U., Yetman, G., Pozzi, F., Hay, S., and Nelson, A., 2006, Determining global population distribution: Methods, applications and data: *Advances in Parasitology*, v. 62, p. 119–156, doi: 10.1016/S0065-308X(05)62004-0.
- Barrie, V., and Greene, G., 2015, Active faulting in the northern Juan de Fuca Strait, Implications for Victoria, British Columbia: *Geological Survey of Canada Current Research 2015-6*, p. 10, doi: 10.4095/296564.
- Blakely, R.J., Wells, R.E., Weaver, C.S., and Johnson, S.Y., 2002, Location, structure, and seismicity of the Seattle fault zone, Washington: Evidence from aeromagnetic anomalies, geologic mapping, and seismic-reflection data: *GSA*

- Bulletin*, v. 114, no. 2, p. 169–177, doi: 10.1130/0016-7606(2002)114<0169:LSASOT>2.0.CO;2.
- Blakely, R.J., Sherrod, B.L., Weaver, C.S., Wells, R.E., and Rohay, A.C., 2014, The Wallula fault and tectonic framework of south-central Washington, as interpreted from magnetic and gravity anomalies: *Tectonophysics*, v. 624–625, p. 32–45, doi: 10.1016/j.tecto.2013.11.006.
- Blyth, H., and Rutter, N., 1993, Surficial geology of the Sooke area (nts 92b/5): British Columbia Ministry of Energy Mines and Petroleum Resources, Open File 1993-25.
- Cassidy, J.F., Rogers, G.C., and Waldhauser, F., 2000, Characterization of active faulting beneath the Strait of Georgia, British Columbia: *Bulletin of the Seismological Society of America*, v. 90, no. 5, p. 1188–1199, doi: 10.1785/0120000044.
- Clague, J.J., and James, T.S., 2002, History and isostatic effects of the last ice sheet in southern British Columbia: *Quaternary Science Reviews*, v. 21, no. 1–3, p. 71–87, doi: 10.1016/S0277-3791(01)00070-1.
- Fairchild, L., and Cowan, D., 1982, Structure, petrology, and tectonic history of the Leech River complex northwest of Victoria, Vancouver Island: *Canadian Journal of Earth Sciences*, v. 19, p. 1817–1835, doi: 10.1139/e82-161.
- Gledhill, K., Ristau, J., Reyners, M., Fry, B., and Holden, C., 2011, The Darfield (Canterbury, New Zealand)  $M_w$  7.1 earthquake of September 2010: A preliminary seismological report: *Seismological Research Letters*, v. 82, no. 3, p. 378–386, doi: 10.1785/gssrl.82.3.378.
- Hetzel, R., and Hampel, A., 2005, Slip rate variations on normal faults during glacial–interglacial changes in surface loads: *Nature*, v. 435, 7038, p. 81–84, doi: 10.1038/nature03562.
- James, T., Bednarski, J., Rogers, G., and Currie, R., 2010, LiDAR and digital aerial imagery of the Leech River Fault Zone and coastal regions from Sombrio Point to Ten Mile Point, southern Vancouver Island, British Columbia: *Geological Survey of Canada, Open-File 6211*, doi: 10.4095/285486.
- Johnson, S., Potter, C., Miller, J., Armentrout, J., Finn, C., and Weaver, C., 1996, The southern Whidbey Island fault: An active structure in the Puget Lowland, Washington: *GSA Bulletin*, v. 108, p. 334–354, doi: 10.1130/0016-7606(1996)108<0334:TSWIFA>2.3.CO;2.
- Johnson, S., Dadisman, S., Mosher, D., Blakely, R., and Childs, J., 2001, Active tectonics of the Devil's Mountain Fault and related structures, Northern Puget Lowland and Eastern Strait of Juan de Fuca Region, Pacific Northwest: U.S. Geological Survey Professional Paper 1643.
- Johnston, S.T., and Acton, S., 2003, The Eocene Southern Vancouver Island Orocline: A response to seamount accretion and the cause of fold-and-thrust belt and extensional basin formation: *Tectonophysics*, v. 365, no. 1–4, p. 165–183, doi: 10.1016/S0040-1951(03)00021-0.
- Johnson, S.Y., Dadisman, S.V., Childs, J.R., and Stanley, W.D., 1999, Active tectonics of the Seattle fault and central Puget Sound, Washington—Implications for earthquake hazards: *GSA Bulletin*, v. 111, no. 7, p. 1042–1053, doi: 10.1130/0016-7606(1999)111<1042:ATOTSF>2.3.CO;2.

- Kelsey, H.M., Sherrod, B.L., Nelson, A.R., and Brocher, T.M., 2008, Earthquakes generated from bedding plane-parallel reverse faults above an active wedge thrust, Seattle fault zone: *GSA Bulletin*, v. 120, no. 11–12, p. 1581–1597, doi: 10.1130/B26282.1.
- Kelsey, H.M., Sherrod, B.L., Blakely, R.J., and Haugerud, R.A., 2012, Holocene faulting in the Bellingham forearc basin: Upper-plate deformation at the northern end of the Cascadia subduction zone: *Journal of Geophysical Research, Solid Earth*, v. 117, B03409, doi: 10.1029/2011JB008816.
- MacLeod, N., Tiffin, D., Snively, P., Jr., and Currie, R., 1977, Geologic interpretation of magnetic and gravity anomalies in the Strait of Juan de Fuca, U.S.–Canada: *Canadian Journal of Earth Sciences*, v. 14, no. 2, p. 223–238, doi: 10.1139/e77-024.
- Massey, N.W.D., MacIntyre, D., Desjardins, P., and Cooney, R., 2005, Digital geology map of British Columbia: BC Ministry of Energy and Mines, Geological Survey Branch, scale: 1:250,000.
- McCaffrey, R., and Goldfinger, C., 1995, Forearc deformation and great subduction earthquakes: Implications for Cascadia offshore earthquake potential: *Science*, v. 267, 5199, p. 856–859, doi: 10.1126/science.267.5199.856.
- McCaffrey, R., King, R.W., Payne, S.J., and Lancaster, M., 2013, Active tectonics of northwestern U.S. inferred from GPS-derived surface velocities: *Journal of Geophysical Research, Solid Earth*, v. 118, p. 709–723, doi: 10.1029/2012JB009473.
- Mosher, D.C., Cassidy, J.F., Lowe, C., Mi, Y., Hyndman, R.D., Rogers, G.C., and Fisher, M., 2000, Neotectonics in the Strait of Georgia: First tentative correlation of seismicity with shallow geological structure in southwestern British Columbia: *Current Research*, p. A22.
- Muller, J.E., 1977, Evolution of the Pacific Margin, Vancouver Island, and adjacent regions: *Canadian Journal of Earth Sciences*, v. 14, no. 9, p. 2062–2085, doi: 10.1139/e77-176.
- Muller, J., 1983, Geology of Victoria map-area: Geological Survey of Canada, “A” Series Map 1553A, 1 sheet, scale: 1:100,000 doi: 10.4095/119507.
- Nelson, A.R., Personius, S.F., Sherrod, B.L., Kelsey, H.M., Johnson, S.Y., Bradley, L.A., and Wells, R.E., 2014, Diverse rupture modes for surface-deforming upper plate earthquakes in the southern Puget Lowland of Washington State: *Geosphere*, v. 10, no. 4, p. 769–796, doi: 10.1130/GES00967.1.
- Personius, S.F., Briggs, R.W., Nelson, A.R., Schermer, E.R., Maharrey, J.Z., Sherrod, B.L., Spaulding, S.A., and Bradley, L.A., 2014, Holocene earthquakes and right-lateral slip on the left-lateral Darrington–Devils Mountain fault zone, northern Puget Sound, Washington: *Geosphere*, v. 10, no. 6, p. 1482–1500, doi: 10.1130/GES01067.1.
- Quigley, M., Van Dissen, R., Litchfield, N., Villamor, P., Duffy, B., Barrell, D., Furlong, K., Stahl, T., Bilderback, E., and Noble, D., 2012, Surface rupture during the 2010  $M_w$  7.1 Darfield (Canterbury) earthquake: Implications for fault rupture dynamics and seismic-hazard analysis: *Geology*, v. 40, no. 1, p. 55–58, doi: 10.1130/G32528.1.
- Rockwell, T., Lindvall, S., Herzberg, M., Murbach, D., Dawson, T., and Berger, G., 2000, Paleoseismology of the Johnson Valley, Kickapoo, and Homestead Valley faults: Clustering of earthquakes in the eastern California shear zone: *Bulletin of the Seismological Society of America*, v. 90, no. 5, p. 1200–1236, doi: 10.1785/0119990023.
- Rogers, G.C., 1988, An assessment of the megathrust earthquake potential of the Cascadia subduction zone: *Canadian Journal of Earth Sciences*, v. 25, no. 6, p. 844–852, doi: 10.1139/e88-083.
- Rusmore, M.E., and Cowan, D.S., 1985, Jurassic-Cretaceous rock units along the southern edge of the Wrangellia terrane on Vancouver Island: *Canadian Journal of Earth Sciences*, v. 22, no. 8, p. 1223–1232, doi: 10.1139/e85-124.
- Sherrod, B., Blakely, R., Weaver, C., Kelsey, H., Barnett, E., Liberty, L., Meagher, K., and Pape, K., 2008, Finding concealed active faults: Extending the southern Whidbey Island fault across the Puget Lowland, Washington: *Journal of Geophysical Research*, v. 113, B05313, doi: 10.1029/2007JB005060.
- Sherrod, B.L., Blakely, R.J., Lasher, J.P., Lamb, A., Mahan, S.A., Foit, F.F., and Barnett, E.A., 2016, Active faulting on the Wallula fault zone within the Olympic-Wallowa lineament, Washington State, USA: *GSA Bulletin*, v. 128, no. 11–12, p. 1636–1659, doi: 10.1130/B31359.1.
- Sylvester, A.G., 1988, Strike-slip faults: *GSA Bulletin*, v. 100, no. 11, p. 1666–1703, doi: 10.1130/0016-7606(1988)100<1666:SSF>2.3.CO;2.
- ten Brink, U., Song, J., and Bucknam, R.C., 2006, Rupture models for the AD 900–930 Seattle fault earthquake from uplifted shorelines: *Geology*, v. 34, no. 7, p. 585–588, doi: 10.1130/G22173.1.
- Thompson, S.C., Weldon, R.J., Rubin, C.M., Abdrakhmatov, K., Molnar, P., and Berger, G.W., 2002, Late Quaternary slip rates across the central Tien Shan, Kyrgyzstan, central Asia: *Journal of Geophysical Research, Solid Earth*, v. 107, no. B9, doi: 10.1029/2001JB000596.
- USGS, 2010, Quaternary fault and fold database for the United States: <http://earthquakes.usgs.gov/hazards/qfaults/> (last accessed April 2015).
- Wells, D.L., and Coppersmith, K.J., 1994, New empirical relationships among magnitude, rupture length, rupture width, rupture area, and surface displacement: *Bulletin of the Seismological Society of America*, v. 84, no. 4, p. 974–1002.
- Wells, R., and Simpson, R., 2001, Northward migration of the Cascadia forearc in the northwestern U.S. and implications for subduction deformation: *Earth, Planets and Space*, v. 53, p. 275–283, doi: 10.1186/BF03352384.

MANUSCRIPT RECEIVED 28 MARCH 2016

REVISED MANUSCRIPT RECEIVED 20 JUNE 2016

MANUSCRIPT ACCEPTED 6 JULY 2016

*The Web of Science's #1 ranked geology journal for 10 years in a row.*

# GEOLOGY

**FREE online access to every  
Geology issue is now included with  
all 2017 GSA Memberships.**

**Not a member? Join Now!** [www.geosociety.org/members/](http://www.geosociety.org/members/)

